Volume 17 | Number 5 | 7 February 2019 | Pages 995–1288

Organic & Biomolecular Chemistry

rsc.li/obc

ISSN 1477-0520

ROYAL SOCIETY OF CHEMISTRY | Celebrating IYPT 2019

COMMUNICATION
Changsheng Zhang *et al.*
Functional characterization of the halogenase SpmH and discovery of new deschloro-tryptophan dimers

Organic & Biomolecular Chemistry

COMMUNICATION

View Article Online
View Journal | View Issue

Cite this: *Org. Biomol. Chem.*, 2019, **17**, 1053

Received 7th November 2018,
Accepted 6th December 2018

DOI: 10.1039/c8ob02775g

rsc.li/obc

Functional characterization of the halogenase SpmH and discovery of new deschloro-tryptophan dimers†

Zhiwen Liu,‡[a] Liang Ma,‡[a] Liping Zhang,[a] Wenjun Zhang,[a] Yiguang Zhu,[a] Yuchan Chen,[b] Weimin Zhang[b] and Changsheng Zhang *[a]

The halogenase gene *spmH* was putatively involved in the biosynthesis of spiroindimicins/indimicins (SPMs/IDMs), a group of chlorinated tryptophan dimers (TDs) from deep-sea-derived *Streptomyces* sp. SCSIO 03032. Inactivation of *spmH* led to six deschloro-analogues of TDs, including four new compounds SPMs G (1) and H (2), and IDMs F (3) and G (4). The structures and absolute configurations of 1–4 were unambiguously determined by the combination of extensive spectroscopic analysis, single-crystal X-ray diffraction and quantum chemical ECD calculations. Compounds 1 and 2 exhibited moderate cytotoxic activities against four cancer cell lines. Additionally, SpmH was biochemically characterized *in vitro* as an L-tryptophan 5-halogenase.

Tryptophan dimers (TDs) are a distinct class of natural products and have attracted significant attention in drug development due to their diverse structures and promising biological activities.[1–3] Several TD analogues are currently in clinical use or clinical trials for cancer therapies.[4,5] For example, midostaurin, featuring a deschloro indolocarbazole scaffold, has been approved by the U.S. Food and Drug Administration for the treatment of FLT3-ITD mutation in acute myeloid leukemia.[6] The biosynthetic studies on TDs have been rigorously carried out during the last two decades to reveal that various skeletons of TDs are derived from the oxidative dimerization of L-tryptophan with further tailoring modifications.[7]

We have previously shown that deep-sea-derived *Streptomyces* sp. SCSIO 03032 could produce a diverse set of unique TDs, such as spiroindimicins (SPMs)[8,9] featuring unique [5,5] or [5,6] spiro-rings, indimicins (IDMs)[10] bearing an unusual dimethyl-hydroindole moiety, and lynamicins (LNMs).[10] *Streptomyces* sp. SCSIO 03032 could also produce piericidins and heronamides (Fig. S1†).[11,12] Recently, a set of biosynthetic genes *spmRAODPFHX2* were identified and characterized to be involved in the biosynthesis of SPMs and IDMs by bioinformatics analysis, targeted gene disruptions, and heterologous expression studies.[13] Similar biosynthetic genes were also found in another marine-derived *Streptomyces* sp. MP131-18.[14] However, key enzymes responsible for assembling the unusual spiro scaffold of SPMs and the dearomatized skeleton of IDMs were indicated to be encoded by genes outside of the identified *spm* gene cluster.[13] Nonetheless, a halogenase SpmH was proposed to catalyze the 5-halogenation of L-tryptophan (L-Trp) to provide the chlorines in SPMs and IDMs.[13] Herein, we report the functional characterization of SpmH as an L-Trp 5-halogenase by *in vivo* gene inactivation experiments and *in vitro* enzyme assays. Seven deschloro metabolites were identified from the Δ*spmH* mutant, including four new TDs, SPMs G (**1**) and H (**2**), and IDMs F (**3**) and G (**4**) (Fig. 1). Biochemically, SpmH was characterized to catalyze the 5-chlorination of L-Trp but not the chlorination of non-halogenated SPM/IDM analogues, suggesting that halogenation occurs as an earlier biosynthetic step in SPMs/IDMs, similar to other halogenated TDs.[15]

Previous bioinformatics analysis showed that SpmH was a putative halogenase with significant similarity to PyrH, an L-Trp 5-halogenase involved in pyrroindomycin biosynthesis.[13,16] To verify its function, the encoding gene *spmH* was inactivated by insertional mutation with an apramycin-resistant gene cassette *via* a PCR-targeting method in *Streptomyces* sp. SCSIO 03032 to afford the Δ*spmH* mutant (Fig. S2†). In comparison with the wild type strain, the Δ*spmH* mutant displayed a different metabolite profile (Fig. 2). Subsequently, 20 L of fermentation cultures of the Δ*spmH* mutant were collected and subjected to acetone extraction and macroporous resin (Amberlite XAD-16) absorption. After multiple steps of chromatographic separation, seven pure compounds (**1–7**) were isolated, including four new compounds SPMs G (**1**) and H (**2**),

[a]*Key Laboratory of Tropical Marine Bio-resources and Ecology, Guangdong Key Laboratory of Marine Materia Medica, RNAM Center for Marine Microbiology, South China Sea Institute of Oceanology, Chinese Academy of Sciences, 164 West Xingang Road, Guangzhou 510301, China. E-mail: czhang2006@gmail.com, czhang@scsio.ac.cn*

[b]*State Key Laboratory of Applied Microbiology Southern China, Guangdong Institute of Microbiology, 100 Central Xianlie Road, Guangzhou 510070, China*

†Electronic supplementary information (ESI) available: The experimental procedures, materials, and characterization of new compounds. CCDC 1873447. For ESI and crystallographic data in CIF or other electronic format see DOI: 10.1039/c8ob02775g

‡These authors contributed equally to this work.

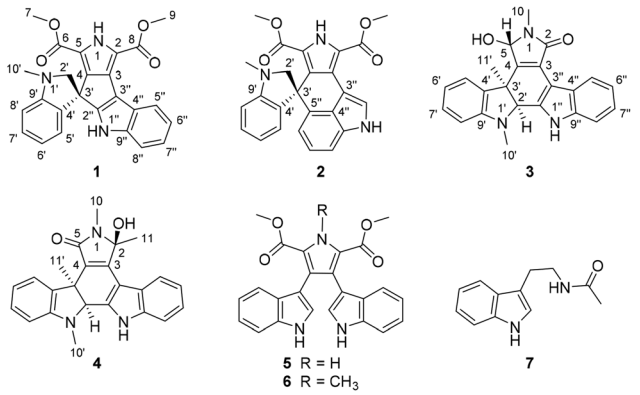

Fig. 1 Chemical structures of compounds **1–7**.

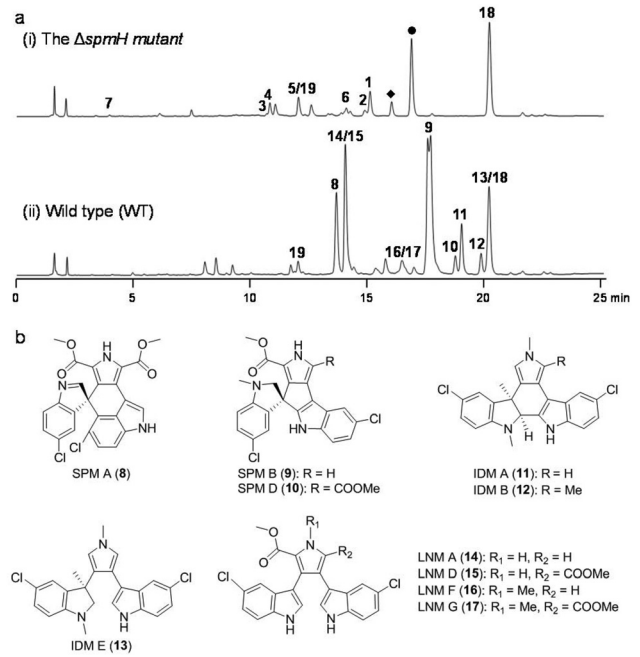

Fig. 2 Comparative HPLC analysis of metabolite profiles (a) and the chemical structures of metabolites from the wild type (WT) strain *Streptomyces* sp. SCSIO 03032 (b). (i) The *spmH* gene inactivation mutant Δ*spmH*; (ii) the wild type strain; UV detection at 254 nm. The compounds denoted by the symbols ■ and ● putatively denoted deschloro-IDM A and deschloro-IDM B, respectively, which were deduced from the UV and mass spectra (Fig. S3†). Both compounds were not subjected to structural elucidation due to instability during isolation. Similarly, previously reported indimicins[10] were also found to be unstable. The structures of piericidin A1 (**18**) and heronamide F (**19**) are shown in Fig. S1.†

and IDMs F (**3**) and G (**4**), and three known deschloro metabolites lycogarubin C (**5**),[17] trimethylated chromopyrrolic acid (**6**),[18] and N_b-acetyl-tryptamine (**7**).[19] The known compounds **5–7** were identified by the comparison of their physical and spectroscopic data in literature reports.[17–19]

SPM G (**1**) was obtained as a white amorphous powder. Its molecular formula was assigned as $C_{25}H_{21}N_3O_4$ by HRESIMS (*m*/*z* 428.1610 $[M + H]^+$, calcd for $C_{25}H_{22}N_3O_4$, 428.1605, Fig. S4†), indicating the presence of 17 degrees of unsaturation. The IR spectrum of **1** (Fig. S4†) displayed absorptions attributable to conjugated carbonyl (1699 cm^{-1}), the double bond (1680 cm^{-1}), and the benzene ring (1603, 1435 cm^{-1}). The NMR spectra of **1** (Table 1 and Fig. S4†), were highly similar to those of SPM D (**10**).[8] A careful comparison revealed that the two chlorines at C-6′ and C-6″ in SPM D (**10**) were absent in **1**, which was supported by its molecular formula and the COSY correlations of H-5′/H-6′/H-7′/H-8′ and H-5″/H-6″/H-7″/H-8″ (Fig. 3). Thus, the planar structure of **1** was determined to be deschloro-SPM D. Based on the good agreement of the electric circular dichroism (ECD) spectra of **1** and **10** (Fig. S4†),[8] the absolute configuration of **1** was deduced to be 3′*R*, the same as that of SPM D (**10**). This assignment was verified by the comparison of the experimental ECD curve of **1** with the calculated ECD curves of two enantiomers (3′*S*)-**1** and (3′*R*)-**1** using the time-dependent density functional theory (TDDFT) at the B3LYP/6-31G (d, p) level.[20] The experimental ECD spectrum of **1** also agreed with the calculated ECD spectrum of (3′*R*)-**1** (Fig. 4a), confirming the absolute configuration of **1** as 3′*R*.

The molecular formula of SPM H (**2**) was assigned to be $C_{25}H_{21}N_3O_4$ by HRESIMS (*m*/*z* 428.1599 $[M + H]^+$, calcd for $C_{25}H_{22}N_3O_4$, 428.1605, Fig. S5†). A comprehensive comparison of the NMR data of **2** (Table 1 and Fig. S5†) and SPM A (**8**)[8] revealed their high similarity. SPM H (**2**) was different from SPM A (**8**) by the presence of characteristic resonances for *N*-methyl (δ_H 2.95, 1H, s; δ_C 35.6), *N*-methylene (δ_H 3.93, 1H, d, J = 8.6 Hz; δ_H 3.83, 1H, d, J = 8.6 Hz; δ_C 74.6), and two *ortho*-disubstituted benzene rings, and the absence of a methylene and two 1,2,4-trisubstituted benzene rings. Based on this comparison, **2** was deduced to be an N-1′ methylated and deschloro derivative of SPM A (**8**). The presence of the N-1′ methyl group was supported by key HMBC correlations from H-2′ to C-10′, and from H-10′ to C-9′. The absence of two chlorines at C-6′ and C-6″ in **2** was supported by the COSY correlations (H-5′/H-6′/H-7′/H-8′ and H-5″/H-6″/H-7″/H-8″) and HMBC correlations (H-6′/C-4′ and H-6″/C-4″). Thus, the planar structure of **2** was determined as shown in Fig. 3. The absolute configuration of **2** was established by comparison of the experimental ECD spectrum of **2** with the calculated ECD spectra of two enantiomers (3′*S*-**2** and 3′*R*-**2**, Fig. 4b). Since the calculated ECD spectrum of (3′*S*)-**2** matched well with the experimental one, the absolute configuration of **2** was assigned to be 3′*S*.

IDM F (**3**) was obtained as colorless block crystals. Its molecular formula of $C_{23}H_{21}N_3O_2$ was established by HRESIMS (*m*/*z* 394.1530 $[M + Na]^+$, calcd for $C_{23}H_{21}N_3O_2Na$, 394.1526, Fig. S6†). Its IR spectrum (Fig. S6†) revealed the absorption bands corresponding to hydroxyl (3362 cm^{-1}), conjugated carbonyl (1688 cm^{-1}) and the benzene ring (1605, 1435 cm^{-1}). A comprehensive analysis of the NMR data of **3** (Table 1 and Fig. S6†) indicated the structure similarity of **3** and IDM A (**11**).[10] The large difference between **3** and IDM A (**11**) was in the pyrrole ring moiety. A 1-methyl-3,4-disubstituted pyrrole ring was present in IDM A (**11**). In contrast, a pyrrolinone unit (**3a**) was established in **3** by HMBC correlations from H-5 to

Table 1 ^{1}H and ^{13}C NMR data of **1–4** (δ in ppm, J in Hz)[a]

	1[b]		**2**[b]		**3**[c]		**4**[b]	
No.	δ_H mult. (J)	δ_C	δ_H mult. (J)	δ_C	δ_H mult. (J)	δ_C	δ_H mult. (J)	δ_C
1 (NH)	9.21 s		9.66 s					
2		113.9		116.7		167.0		87.7
3		133.6		123.9		127.2		149.2
4		140.8		132.0		145.7		125.4
5		119.8		123.0	4.83 d (8.8)	83.0		168.1
6		161.2		161.0				
7	4.08 s	52.0	3.49 s	51.9				
8		160.2		160.4				
9	3.60 s	51.6	4.02 s	51.6				
10					2.80 s	25.5	2.88 s	22.2
11							1.72 s	22.9
2′	(a) 4.01 d (8.7) (b) 3.59 d (8.7)	64.1	(a) 3.93 d (8.6) (b) 3.83 d (8.6)	74.6	4.12 s	71.2	4.07 s	72.4
3′		51.9		49.2		46.5		46.5
4′		131.6		141.1		132.4		131.7
5′	6.57	122.9	6.52 d (7.3)	123.4	7.40 d (7.5)	123.9	7.95 dd (7.5, 1.0)	127.6
6′	6.58	119.0	6.47 dd (7.3, 7.3)	117.7	6.81 dd (7.5, 7.5)	118.8	6.85 ddd (7.5, 7.5, 1.0)	119.4
7′	7.14 dd (7.9, 7.9)	128.7	7.09 dd (7.3, 7.3)	127.5	7.11	127.7	7.12 ddd (7.5, 7.5, 1.0)	127.8
8′	6.70 d (7.9)	108.4	6.64 d (7.3)	106.3	6.58 d (7.5)	107.5	6.50 dd (7.5, 1.0)	107.5
9′		153.6		152.7		152.5		152.2
10′	2.90 s	36.7	2.95 s	35.6	2.72 s	34.5	2.78 s	35.5
11′					1.54 s	22.9	1.59 s	24.1
1″ (NH)	8.58 s		8.15 br s		11.9 s		8.89 s	
2″		156.8	7.97 d (2.2)	121.3		133.1		135.8
3″		111.6		106.6		103.9		106.1
4″		121.9		123.3		123.3		123.2
5″	8.18 d (7.8)	120.9		137.3	8.45 d (8.0)	122.5	8.24 d (7.7)	122.2
6″	7.20 dd (7.8, 7.8)	121.0	7.05 d (7.6)	116.8	7.07 dd (8.0, 8.0)	119.8	7.24 dd (7.7, 7.7)	121.7
7″	7.16 dd (7.8, 7.8)	122.0	7.14 dd (7.6, 7.6)	125.1	7.13	121.5	7.29 dd (7.7, 7.7)	123.1
8″	7.24 d (7.8)	112.1	7.17 d (7.6)	108.4	7.44 d (8.0)	111.7	7.46 d (7.7)	111.8
9″		140.0		134.1		136.4		136.8
OH					6.49 d (8.8)			

[a] Spectra recorded at 500 MHz for ^{1}H NMR and 125 MHz for ^{13}C NMR; overlapped signals are reported without designating multiplicity. [b] Measured in $CDCl_3$. [c] Measured in DMSO-d_6.

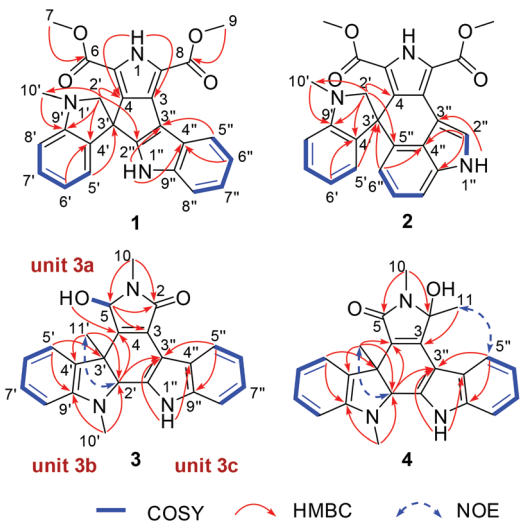

Fig. 3 ^{1}H–^{1}H COSY, key HMBC and NOESY correlations of **1–4**.

C-2/C-3, and from H-6 to C-2/C-5, and COSY correlations between H-5/5-OH. Compound **3** also exhibited NMR signals for two *ortho*-disubstituted benzene rings (Table 1), indicating that **3** was a 6′,6″-dideschloro-derivative of IDM A (**11**). This assignment was supported by the COSY correlations of H-5′/H-6′/H-7′/H-8′ and H-5″/H-6″/H-7″/H-8″ (Fig. 3). Other key HMBC correlations assembled the units **3b** and **3c** (Fig. 3 and Table 1). The connection of units **3a**/**3b**/**3c** through C-4/C-3′ and C2′/C-2″ was supported by HMBC correlations from H-2′ to C-4/C-3″ and from Me-11′ to C-4. The NOESY correlation of Me-11′/H-2′ was observed (Fig. 3), placing these protons at the same side of the 5 membered ring in unit **3b**. Finally, a crystal of **3** was obtained for single-crystal X-ray diffraction with Cu Kα radiation (CCDC 1873447†), allowing unambiguous assignment of its absolute configuration as 5*S*,2′*S*,3′*S* (Fig. 5) with a Flack parameter of 0.05(7).

The molecular formula of IDM G (**4**) was determined as $C_{24}H_{23}N_3O_2$ by HRESIMS (m/z 384.1718 $[M - H]^-$, calcd for $C_{24}H_{22}N_3O_2$, 384.1722, Fig. S7†). The 1D NMR spectra of **4** and **3** were very similar (Table 1 and Fig. S7†). IDM G (**4**) only differed from **3** in the substituted pyrrolinone moiety: (1) the keto group was located at C-5 (δ_C 168.1) in **4**, instead of being at C-2 in **3** (δ_C 83.0); (2) a tertiary methyl (δ_H 1.72, 3H, s; δ_C 22.9) was placed at the hydroxylated quaternary carbon C-2 (δ_C 87.7, C-2), which was confirmed by HMBC correlations from Me-11 to C-3 and from Me-10 to C-5/C-2, and further supported by the NOE correlation between Me-11 and H-5″

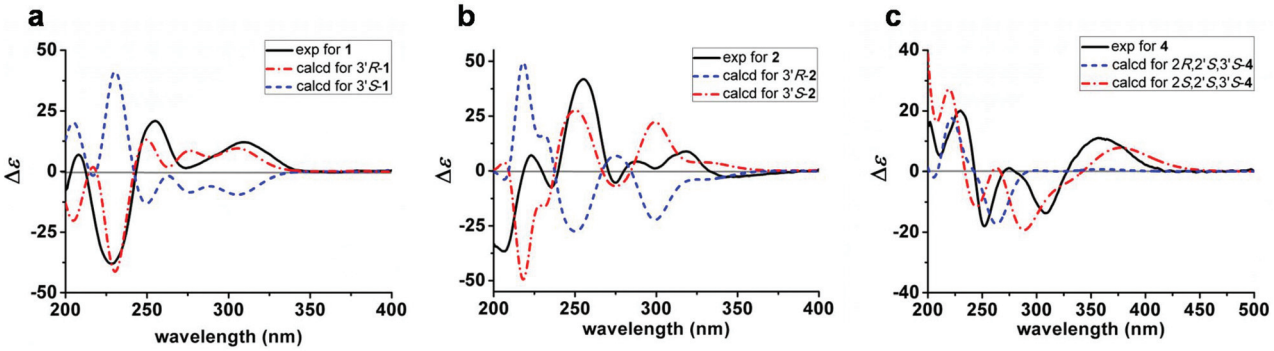

Fig. 4 Experimental (exp.) and calculated (calcd) ECD spectra of **1** (a), **2** (b) and **4** (c).

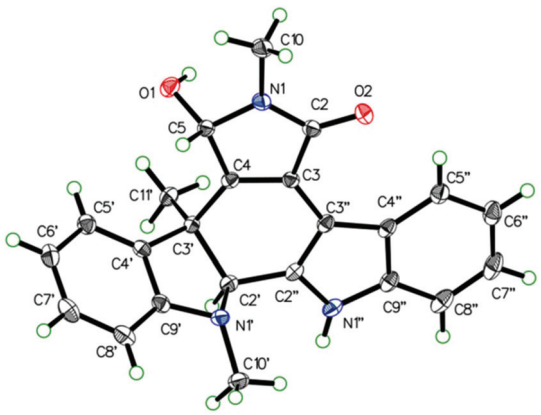

Fig. 5 X-ray crystallographic structures of **3**.

(Fig. 3). In contrast, a hydroxyl methine was present at C-5 in **3**. The *syn* configuration of Me-11′ and H-2′ was assigned by the key NOE correlation of Me-11′/H-2′ (Fig. 3). Based on the same biosynthetic origin of **3** and **4**, the absolute configurations of C-2′ and C-3′ in **4** were deduced as 2′*S*,3′*S*. Finally, the absolute configuration of **4** was determined to be 2*S*,2′*S*,3′*S* by comparison of the experimental ECD curve **4** with the calculated ECD curves of two possible configurations (2*S*,2′*S*,3′*S* and 2*R*,2′*S*,3′*S*; Fig. 4c).

Compounds **1**–**7** were evaluated for their *in vitro* cytotoxicity against four cancer cell lines (SF-268, MCF-7, HepG2 and A549). It was shown that **1** and **2** exhibited moderate cytotoxic effects against the four cancer cell lines, comparable to their chlorinated analogues SPMs A (**8**) and D (**10**) (Table 2).[8] This observation indicated that chlorination of SPMs exerted little effects on the cytotoxicity.

Our *in vivo* data suggested that SpmH was a halogenase. To probe its function and substrates *in vitro*, SpmH was overproduced in *E. coli* BL21(DE3) and purified as a soluble His_6-tagged protein (Fig. S11†). Subsequent incubation of L-Trp (**20**) and SpmH led to the conversion of L-Trp (**20**) to **21** (Fig. 6, trace i), in the presence of NaCl, flavin adenine dinucleotide (FAD), and dithiothreitol (DTT, a redox reagent to *in situ* reduce FAD to $FADH_2$,[21,22] Fig. 6). Product **21** was characterized as 5-Cl-L-Trp by comparison of the UV/ESIMS spectra and the retention time with the standard (Fig. S12 and 13†).

Table 2 Cytotoxic activities of compounds **1** and **2**

	IC_{50} (μM)			
Compd	SF-268	MCF-7	HepG2	A549
SPM G (**1**)	16.09 ± 1.26	19.11 ± 2.23	13.57 ± 0.24	10.28 ± 0.14
SPM H (**2**)	23.54 ± 0.29	33.02 ± 3.41	20.92 ± 0.69	18.16 ± 0.59
SPM A (**8**)	18.72 ± 0.29	25.09 ± 0.58	21.21 ± 1.01	21.62 ± 0.66
SPM D (**10**)	20.73 ± 1.67	14.61 ± 0.46	7.05 ± 0.53	19.50 ± 0.96
Adriamycin	0.57 ± 0.04	0.95 ± 0.06	1.18 ± 0.15	0.78 ± 0.05

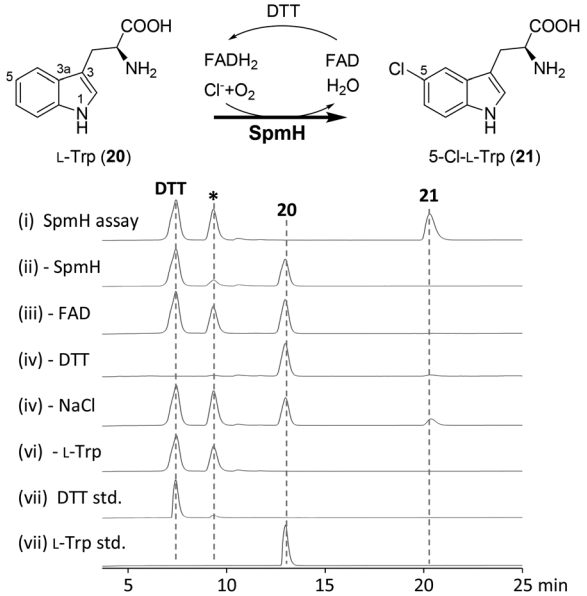

Fig. 6 The scheme of SpmH-catalyzed halogenation and HPLC analysis of enzyme assays, UV detection at 220 nm. (i) A typical *in vitro* SpmH assay was conducted in 100 μL of the reaction mixture in potassium phosphate buffer (50 mM, pH 7.4), comprising 150 μM L-Trp (**20**), 5 μM SpmH, 10 μM FAD, 20 mM DTT and 50 mM NaCl at 30 °C for 12 h; (ii) minus SpmH, (iii) minus FAD, (iv) minus DTT, (v) minus NaCl, (vi) minus L-Trp (**20**), (vii) DTT standard, and (viii) L-Trp (**20**) standard. The peak with an asterisk symbol denotes an unknown product derived from the oxidation of DTT.

Further experiments showed that the yield of product **21** increased with a longer incubation time in a typical SpmH enzyme assay (Fig. S13†). No conversion of L-Trp (**20**) was observed in control assays lacking either SpmH or FAD (Fig. 6, traces ii & iii). A trace amount of product **21** was observed in assays lacking DTT (Fig. 6, trace iv) or lacking NaCl (Fig. 6, trace v) due to the presence of DDT and Cl^- in the storage buffer and the protein purification system.[16,23] However, none of the compounds **1–7** were detected as putative substrates for SpmH (Fig. S14†). These observations unequivocally confirmed that SpmH catalyzed the conversion of L-Trp (**20**) to 5-Cl-L-Trp (**21**) during the early steps in the biosynthesis of SPMs/IDMs.

Conclusions

In summary, four new TDs, SPMs G (**1**) and H (**2**), and IDMs F (**3**) and G (**4**), together with 3 known compounds **5–7** were isolated from the *spmH* gene inactivation mutant of *Streptomyces* sp. SCSIO 03032. The structure elucidation of these metabolites demonstrated that they were deschloro-analogues of SPM/IDMs. SPMs **1** and **2** exhibited moderate cytotoxic effects against four cancer cell lines. Subsequently, *in vitro* enzyme assays demonstrated that the flavin-dependent enzyme SpmH was an L-Trp 5-halogenase, while deschloro SPMs/IDMs were not substrates for SpmH. Our study highlights the inactivation of functional biosynthetic genes in marine actinomycetes as an effective strategy for the discovery of novel natural products.

Conflicts of interest

There are no conflicts to declare.

Acknowledgements

This work was financially supported by grants from the NSFC (31470172), the Chinese Academy of Sciences (QYZDJ-SSW-DQC004), the Natural Science Foundation of Guangxi Province (2016GXNSFBA380095), and the China Postdoctoral Science Foundation (2018M643230). We are grateful for the analytical facility in the South China Sea Institute of Oceanology for recording spectroscopic data and the high-performance computing platform of Jinan University for ECD calculations.

Notes and references

1 Y. L. Du and K. S. Ryan, *Curr. Opin. Chem. Biol.*, 2016, **31**, 74–81.
2 S. B. Bharate, S. D. Sawant, P. P. Singh and R. A. Vishwakarma, *Chem. Rev.*, 2013, **113**, 6761–6815.
3 M. Prudhomme, *Eur. J. Med. Chem.*, 2003, **38**, 123–140.
4 A. Dowlati, J. Posey, R. K. Ramanathan, L. Rath, P. Fu, A. Chak, S. Krishnamurthi, J. Brell, S. Ingalls, C. L. Hoppel, P. Ivy and S. C. Remick, *Cancer Chemother. Pharmacol.*, 2009, **65**, 73–78.
5 T. Fischer, R. M. Stone, D. J. Deangelo, I. Galinsky, E. Estey, C. Lanza, E. Fox, G. Ehninger, E. J. Feldman, G. J. Schiller, V. M. Klimek, S. D. Nimer, D. G. Gilliland, C. Dutreix, A. Huntsman-Labed, J. Virkus and F. J. Giles, *J. Clin. Oncol.*, 2010, **28**, 4339–4345.
6 R. M. Stone, S. J. Mandrekar, B. L. Sanford, K. Laumann, S. Geyer, C. D. Bloomfield, C. Thiede, T. W. Prior, K. Dohner, G. Marcucci, F. Lo-Coco, R. B. Klisovic, A. Wei, J. Sierra, M. A. Sanz, J. M. Brandwein, T. de Witte, D. Niederwieser, F. R. Appelbaum, B. C. Medeiros, M. S. Tallman, J. Krauter, R. F. Schlenk, A. Ganser, H. Serve, G. Ehninger, S. Amadori, R. A. Larson and H. Dohner, *N. Engl. J. Med.*, 2017, **377**, 454–464.
7 L. M. Alkhalaf and K. S. Ryan, *Chem. Biol.*, 2015, **22**, 317–328.
8 W. Zhang, Z. Liu, S. Li, T. Yang, Q. Zhang, L. Ma, X. Tian, H. Zhang, C. Huang, S. Zhang, J. Ju, Y. Shen and C. Zhang, *Org. Lett.*, 2012, **14**, 3364–3367.
9 L. M. Blair and J. Sperry, *Chem. Commun.*, 2016, **52**, 800–802.
10 W. Zhang, S. Li, Y. Zhu, Y. Chen, H. Zhang, G. Zhang, X. Tian, Y. Pan, S. Zhang and C. Zhang, *J. Nat. Prod.*, 2014, **77**, 388–391.
11 Y. Chen, W. Zhang, Y. Zhu, Q. Zhang, X. Tian, S. Zhang and C. Zhang, *Org. Lett.*, 2014, **16**, 736–739.
12 Y. Zhu, W. Zhang, Y. Chen, C. Yuan, H. Zhang, G. Zhang, L. Ma, Q. Zhang, X. Tian, S. Zhang and C. Zhang, *ChemBioChem*, 2015, **16**, 2086–2093.
13 L. Ma, W. Zhang, Y. Zhu, G. Zhang, H. Zhang, Q. Zhang, L. Zhang, C. Yuan and C. Zhang, *Appl. Microbiol. Biotechnol.*, 2017, **101**, 6123–6136.
14 C. Paulus, Y. Rebets, B. Tokovenko, S. Nadmid, L. P. Terekhova, M. Myronovskyi, S. B. Zotchev, C. Ruckert, S. Braig, S. Zahler, J. Kalinowski and A. Luzhetskyy, *Sci. Rep.*, 2017, **7**, 42382.
15 E. Yeh, L. J. Cole, J. M. Bollinger Jr., D. P. Ballou and C. T. Walsh, *Biochemistry*, 2006, **45**, 7904–7912.
16 S. Zehner, A. Kotzsch, B. Bister, R. D. Sussmuth, C. Mendez, J. A. Salas and K. H. van Pee, *Chem. Biol.*, 2005, **12**, 445–452.
17 K. A. McArthur, S. S. Mitchell, G. Tsueng, A. Rheingold, D. J. White, J. Grodberg, K. S. Lam and B. C. M. Potts, *J. Nat. Prod.*, 2008, **71**, 1732–1737.
18 T. Hoshino, Y. O. Kojima, T. Hayashi, T. Uchiyama and K. Kaneko, *Biosci., Biotechnol., Biochem.*, 2014, **57**, 775–781.
19 Y. Li, X. F. Li, D. S. Kim, H. D. Choi and B. W. Son, *Arch. Pharmacal Res.*, 2003, **26**, 21–23.
20 A. E. Nugroho and H. Morita, *J. Nat. Med.*, 2014, **68**, 1–10.
21 E. Gross, D. B. Kastner, C. A. Kaiser and D. Fass, *Cell*, 2004, **117**, 601–610.
22 E. Bitto, Y. Huang, C. A. Bingman, S. Singh, J. S. Thorson and G. N. Phillips, *Proteins*, 2008, **70**, 289–293.
23 J. Zeng and J. Zhan, *ChemBioChem*, 2010, **11**, 2119–2123.